

Radiative decay of the sub-threshold 1_1^- and 2_1^+ states of ^{16}O in cluster effective field theory

Shung-Ichi Ando¹,

Department of Display and Semiconductor Technology, Sunmoon University, Asan, Chungnam 31460, Republic of Korea

Radiative decay of the sub-threshold 1_1^- and 2_1^+ states of ^{16}O is studied in cluster effective field theory. The wave function normalization factors for initial and final states of the radiative decay amplitudes are deduced by using the phase shift data of elastic α - ^{12}C scattering for $l = 0, 1, 2$, which are related to the asymptotic normalization coefficients of 0_1^+ , 1_1^- , 2_1^+ states of ^{16}O for the two-body α - ^{12}C channel; then only one unfixed parameter remains in each of the radiative decay amplitudes. We fit the parameters to the experimental radiative decay rates and apply the fitted parameters to the study of radiative α capture on ^{12}C , $^{12}\text{C}(\alpha, \gamma)^{16}\text{O}$. The order of magnitude of astrophysical S factors of $E1$ and $E2$ transitions of $^{12}\text{C}(\alpha, \gamma)^{16}\text{O}$ is reproduced compared to the experimental data, and we discuss an improvement in the calculation of S factors of $^{12}\text{C}(\alpha, \gamma)^{16}\text{O}$.

PACS(s): 11.10.Ef, 24.10.-i, 25.55.-e, 26.20.Fj

¹<mailto:sando@sunmoon.ac.kr>

1. Introduction

The radiative α capture on ^{12}C , $^{12}\text{C}(\alpha,\gamma)^{16}\text{O}$, is a fundamental reaction in nuclear astrophysics, which determines, together with the triple α process, the C/O ratio in the core of a helium-burning star [1]. It plays a crucial role in simulations of nucleosynthesis in star evolutions [2, 3], e.g., the radiative α capture reaction is one of the most uncertain nuclear processes in different models of type Ia Supernova nucleosynthesis [4]. The α capture rate, or alternatively the astrophysical S factor of $^{12}\text{C}(\alpha,\gamma)^{16}\text{O}$ at the energy of helium-burning process, namely the Gamow-peak energy, $E_G = 0.3$ MeV, has never been measured in an experimental facility because of the Coulomb barrier. One needs to employ a theoretical model, whose parameters are fitted to experimental data measured at a few MeV energy, and extrapolate the reaction rate down to E_G . During the last half-century, many experimental and theoretical studies have been carried out; refer to, e.g., Refs. [5, 6, 7, 8, 9] for review.

During the last decade, we have been studying an estimate of the S factor of $^{12}\text{C}(\alpha,\gamma)^{16}\text{O}$ by employing the methodology of effective field theory (EFT) [10, 11, 12]. An EFT is constructed by introducing a scale that separates relevant degrees of freedom at low energy from irrelevant degrees of freedom at high energy. Then, one constructs the most general form of effective Lagrangian so as to satisfy the symmetry requirement and expands it in powers of the number of derivatives; the theory provides us with a perturbative expansion scheme in terms of Q/Λ_H where Q is a typical momentum scale of a reaction in question and Λ_H is a momentum scale of high energy for separation. The irrelevant degrees of freedom are integrated out of the Lagrangian and their effect is embedded in the coefficients of terms of Lagrangian. Those coefficients, in principle, can be determined within its mother theory while they, in practice, are fixed by using empirical values or fitted to experimental data. Furthermore, the inclusion of a resonance state in theory was studied by, e.g., Galman [13] and Habashi, Fleming, and van Kolck [14]. EFTs are applied to various studies for nuclear reactions at low energies, such as radiative neutron capture on a proton for big-bang nucleosynthesis [15, 16, 17], proton-proton capture in hydrogen burning [18, 19, 20], and solar neutrino reactions on a deuteron [21, 22].

To construct an EFT for the calculation of the astrophysical S factor of $^{12}\text{C}(\alpha,\gamma)^{16}\text{O}$ at E_G , we choose the energy difference between the open channels of α - ^{12}C and p - ^{15}N states, $\Delta E = 4$ MeV, for the separation scale, and one has the large momentum scale Λ_H as $\Lambda_H = \sqrt{2\mu\Delta E} = 160$ MeV where μ is the reduced mass of α and ^{12}C . The relevant degrees of freedom for the theory are α and ^{12}C represented as non-relativistic point-like scalar fields. The effective Lagrangian is constructed so as to be invariant under the Galilean and gauge transformations, and expanded in terms of the number of covariant derivatives. The typical momentum scale at E_G is $Q = \sqrt{2\mu E_G} = 40$ MeV, and the expansion parameter becomes $Q/\Lambda_H = 1/4$. We introduce auxiliary fields for bound and resonant states of ^{16}O to carry out a momentum expansion around the unitary limit [23, 24, 25], which reproduces the expression of effective range expansion [26]. In addition, it is straightforward to introduce the electromagnetic and weak interactions in the theory. In the previous works, we constructed an EFT for an estimate of S factor of $^{12}\text{C}(\alpha,\gamma)^{16}\text{O}$ at E_G studying elastic α - ^{12}C scattering for various cases of including the

bound and resonant states of ^{16}O [27, 28, 29, 30], $E1$ transition of $^{12}\text{C}(\alpha,\gamma)^{16}\text{O}$ [31], and β delayed α emission from ^{16}N [9].

In this work, we study the radiative decay of excited 1_1^- and 2_1^+ states of ^{16}O within the cluster EFT. The main aim of the present work is to seek constraints on the radiative capture amplitudes of $^{12}\text{C}(\alpha,\gamma)^{16}\text{O}$. Feynman diagrams of the radiative decay process are parts of those of $^{12}\text{C}(\alpha,\gamma)^{16}\text{O}$, and one can fix the coupling constants of $O^*\gamma O$ vertex functions by using the experimental data of decay rates of 1_1^- and 2_1^+ states of ^{16}O . We also employ the wave function normalization factors, equivalently the asymptotic normalization coefficients (ANCs) of 0_1^+ , 1_1^- , 2_1^+ states of ^{16}O , to fix the coupling constants of αCO vertex function for the final 0_1^+ ground state of ^{16}O and $O^*\alpha C$ vertex functions for the initial 1_1^- and 2_1^+ states of ^{16}O . Moreover, we improve the regularization method for logarithmic divergence appearing from loop diagrams. In the previous work [31], we employed two regularization methods, sharp cutoff regularization and dimensional regularization. In this work, we apply the dimensional regularization method to the calculation of logarithmic divergence, which previously was regularized by introducing a sharp cutoff. Then, we fit the couplings of $O^*\gamma O$ vertex functions to the experimental data of decay rates of 1_1^- and 2_1^+ states of ^{16}O as functions of the sharp cutoff parameter r_C ; a mild cutoff dependence is found compared to the result in the previous study [31]. Now there are no free parameters in the amplitudes of $^{12}\text{C}(\alpha,\gamma)^{16}\text{O}$. We calculate the S factors of $E1$ and $E2$ transitions of $^{12}\text{C}(\alpha,\gamma)^{16}\text{O}$ by using the fitted parameters and plot the curves of S factors with the experimental data. We find that the order of magnitude of S factors is reproduced and discuss how the calculation of S factors of $^{12}\text{C}(\alpha,\gamma)^{16}\text{O}$ can be improved.

The present work is organized as follows. In Sec. 2 the expression of effective Lagrangian is reviewed, and in Sec. 3, the radiative decay amplitudes are derived considering the regularization methods of loop diagrams and the wave function normalization factors, equivalently the ANCs of 0_1^+ , 1_1^- , 2_1^+ states of ^{16}O . In Sec. 4, the numerical results of fitting the parameters and plotting the S factors of $^{12}\text{C}(\alpha,\gamma)^{16}\text{O}$ are discussed, and finally in Sec. 5, the results and discussion of this work are presented. In Appendix A, masses and formulae of the decay rates for the present study are summarized, and in Appendix B, the derivation of ANC of ground 0_1^+ state of ^{16}O from the phase shift of elastic α - ^{12}C scattering is discussed.

2. Effective Lagrangian

As discussed in the introduction, the theory has a perturbative scheme in terms of the number of derivatives: the expansion parameter is obtained as $Q/\Lambda_H = 1/4$. While we discussed a modification of the counting rules for the effective range expansion for elastic α - ^{12}C scattering at low energies [28]; one or two orders of magnitude larger contributions (than the term estimated by using a phase shift datum at the lowest energy in the experiment [35]²) appear from the Coulomb self-energy term. To subtract those unnaturally large contributions, we include the effective range terms up to p^6 order as counter terms.

²The lowest energy of the experimental data for the elastic α - ^{12}C scattering is $E_\alpha = 2.6$ MeV where E_α is the α energy in the lab frame.

In the study of $E1$ transition of $^{12}\text{C}(\alpha,\gamma)^{16}\text{O}$, on the other hand, it is known that the $E1$ transition is suppressed between initial and final isospin singlet states. The suppression factor can be seen in the term, $(Z_\alpha/m_\alpha - Z_C/m_C)$, in the amplitudes, where Z_α and m_α (Z_C and m_C) are the proton number and mass of α (^{12}C); if one ignores the binding energies of nuclei, $m_\alpha \simeq 4m_N$ and $m_C \simeq 12m_N$ where m_N is the nucleon mass, and $Z_\alpha = 2$ and $Z_C = 8$, the term $(Z_\alpha/m_\alpha - Z_C/m_C)$ vanishes. The prime contribution to the $E1$ transition amplitudes comes out of the coupling constant of $O^*\gamma O$ vertex function. This constant is supposed to contain dynamics from high energy: a significant contribution may come out of the isovector channel, namely, p - ^{15}N state. The p - ^{15}N open channel can appear in loop diagrams instead of α - ^{12}C state. While the p - ^{15}N state is integrated out and its effect is embedded in the coupling constant of $O^*\gamma O$ vertex function; we fitted the coupling constant to experimental data of S factor for $E1$ transition of $^{12}\text{C}(\alpha,\gamma)^{16}\text{O}$ in the previous study [31].

The effective Lagrangian for radiative decay of 1^- and 2_1^+ states of ^{16}O is the same as that for $E1$ and $E2$ transitions of $^{12}\text{C}(\alpha,\gamma)^{16}\text{O}$ [31]. Thus, one has

$$\begin{aligned}
\mathcal{L} = & \phi_\alpha^\dagger \left(iD_0 + \frac{\vec{D}^2}{2m_\alpha} + \dots \right) \phi_\alpha + \phi_C^\dagger \left(iD_0 + \frac{\vec{D}^2}{2m_C} + \dots \right) \phi_C \\
& + \sum_{n=0}^3 C_n^{(0)} d^\dagger \left[iD_0 + \frac{\vec{D}^2}{2(m_\alpha + m_C)} \right]^n d - y^{(0)} \left[d^\dagger (\phi_\alpha \phi_C) + (\phi_\alpha \phi_C)^\dagger d \right] \\
& + \sum_{n=0}^3 C_n^{(1)} d_i^\dagger \left[iD_0 + \frac{\vec{D}^2}{2(m_\alpha + m_C)} \right]^n d_i - y^{(1)} \left[d_i^\dagger (\phi_\alpha O_i^{(1)} \phi_C) + (\phi_\alpha O_i^{(1)} \phi_C)^\dagger d_i \right] \\
& + \sum_{n=0}^3 C_n^{(2)} d_{ij}^\dagger \left[iD_0 + \frac{\vec{D}^2}{2(m_\alpha + m_C)} \right]^n d_{ij} - y^{(2)} \left[d_{ij}^\dagger (\phi_\alpha O_{ij}^{(2)} \phi_C) + (\phi_\alpha O_{ij}^{(2)} \phi_C)^\dagger d_{ij} \right] \\
& - h^{(1)} \frac{y^{(0)} y^{(1)}}{\mu} \left[(\mathcal{O}_l^{(1)} d)^\dagger d_l + \text{H.c.} \right] - h^{(2)} \frac{y^{(0)} y^{(2)}}{\mu^2} \left[(\mathcal{O}_{ij}^{(2)} d)^\dagger d_{ij} + \text{H.c.} \right] + \dots, \quad (1)
\end{aligned}$$

where ϕ_α (m_α) and ϕ_C (m_C) are fields (masses) of α and ^{12}C , respectively. D_μ is the covariant derivative, $D_\mu \phi = (\partial_\mu + ieZA_\mu)\phi$, where e is the electric charge, Z is the number of protons in a nucleus, and A_μ is the photon field. The combination of the terms, $iD_0 + \vec{D}^2/(2m)$, is required for the invariance under the Galilean transformation. The dots denote higher-order terms. d , d_i , d_{ij} are fields of composite states of α and ^{12}C for $l = 0, 1, 2$, respectively, which represent the bound states of ^{16}O ³, where the spin states are represented as Cartesian tensors of rank l . The coefficients $C_n^{(l)}$ correspond with the effective range parameters in the form of $C_n^{(l)}/y^{(l)2}$ with $l = 0, 1, 2$, where $y^{(l)}$ are the coupling constants of $O^*\alpha C$ and $O\alpha C$ vertex functions. As mentioned before, we include the effective range parameters up to p^6 order; namely, $n = 0, 1, 2, 3$. $h^{(1)}$ and $h^{(2)}$ are bare

³We suppress the terms of Lagrangian for resonance states of ^{16}O for the sake of simplicity, which are involved when fitting the phase shift data of elastic α - ^{12}C scattering. One can find the expression of the terms in Eq. (6) in Ref. [30].

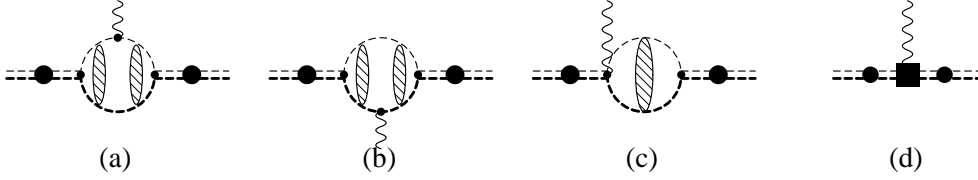


Figure 1: Diagrams of radiative decay amplitudes for $^{16}\text{O}^*(1_1^-) \rightarrow ^{16}\text{O}_{g.s.} + \gamma$ and $^{16}\text{O}^*(2_1^+) \rightarrow ^{16}\text{O}_{g.s.} + \gamma$. A thick (thin) dashed line represents a propagator of ^{12}C (α), and a thick and thin double-dashed line with a filled circle represents the initial and final states of ^{16}O , and a wavy line the outgoing photon. A shaded blob represents a set of diagrams consisting of all possible one-potential-photon-exchange diagrams up to infinite order and no potential-photon-exchange one, namely, the Coulomb greens function. A filled box represents the contact interactions of $O^*\gamma O$ vertex functions and renormalize the divergence terms from the loop diagrams.

coupling constants of contact $O^*\gamma O$ vertex functions, with which the infinities from loop diagrams are renormalized. The projection operators in p -wave and d -wave read

$$O_i^{(1)} = i \frac{\overleftrightarrow{D}_i}{M} \equiv i \left(\frac{\overrightarrow{D}_C}{m_C} - \frac{\overleftarrow{D}_\alpha}{m_\alpha} \right)_i, \quad O_{ij}^{(2)} = -\frac{\overleftrightarrow{D}_i \overleftrightarrow{D}_j}{M M} + \frac{1}{3} \delta_{ij} \frac{\overleftrightarrow{D}^2}{M^2}, \quad (2)$$

$$O_i^{(1)} = \frac{i D_i}{m_O}, \quad O_{ij}^{(2)} = -\frac{1}{m_O^2} (D_i D_j - \frac{1}{3} \delta_{ij} D^2), \quad (3)$$

where m_O is the mass of ground 0_1^+ state of ^{16}O .

3. Radiative decay amplitudes

In this section, we derive expressions of the decay amplitudes from the effective Lagrangian. We discuss an improvement in regularization methods of the log divergence from loop diagrams and the calculation of wave function normalization factors by using the phase shift data of elastic α - ^{12}C scattering; final expressions of the decay amplitudes of 1_1^- and 2_1^+ states of ^{16}O contain only one parameter for each of the amplitudes, and the parameters are fitted to the experimental decay rates in the next section.

3.1 Amplitudes

The radiative decay amplitudes $A^{(l)}$ with $l = 1, 2$ are calculated from diagrams displayed in Fig. 1, which are parts of the diagrams for $^{12}\text{C}(\alpha, \gamma)^{16}\text{O}$ (displayed in Fig. 2 in Ref. [31]). The amplitudes $A^{(l)}$ with $l = 1, 2$ are represented as

$$A^{(l=1)} = \vec{\epsilon}_{(\gamma)}^* \cdot \vec{\epsilon}_{(l=1)} Y^{(l=1)}, \quad (4)$$

$$A^{(l=2)} = \epsilon_{(\gamma)}^{*i} \hat{k}_2^j \epsilon_{(l=2)}^{ij} Y^{(l=2)}, \quad (5)$$

with

$$Y^{(l)} = Y_{(a+b)}^{(l)} + Y_{(c)}^{(l)} + Y_{(d)}^{(l)}, \quad (6)$$

where $\vec{\epsilon}_{(\gamma)}^*$ is the polarization vector of out-going photon, $\vec{\epsilon}_{(l=1)}$ is the polarization vector of initial p -wave state of $^{16}\text{O}^*(1_1^-)$, and \hat{k}_2 is a unit vector of the momentum \vec{k}_2 of out-going photon from the decay of 2_1^+ state of ^{16}O , and $\epsilon_{(l=2)}^{ij}$ is the symmetric traceless tensor of initial d -wave state of $^{16}\text{O}^*(2_1^+)$. The amplitudes, $Y_{(a+b)}^{(l)}$, $Y_{(c)}^{(l)}$, $Y_{(d)}^{(l)}$, correspond to the diagrams displayed in Fig. 1. Masses and decay rates for the present study are summarized in Appendix A. Thus, the spin-averaged decay rates in Eq. (45) become

$$\Gamma^{(l=1)} = \frac{\alpha_E k_1}{3\pi} |Y^{(l=1)}|^2, \quad (7)$$

$$\Gamma^{(l=2)} = \frac{\alpha_E k_2}{5\pi} |Y^{(l=2)}|^2, \quad (8)$$

where α_E is the fine structure constant, and k_1 and k_2 are the magnitude of photon momenta in Eqs. (43) and (44) for radiative decay of 1_1^- and 2_1^+ states of ^{16}O , respectively. The amplitudes, $Y_{(a+b)}^{(l)}$, $Y_{(c)}^{(l)}$, and $Y_{(d)}^{(l)}$, are obtained as

$$\begin{aligned} Y_{(a+b)}^{(l=1)} &= +\frac{1}{9\pi} y^{(0)} y^{(1)} \gamma_1 \Gamma(1 + \kappa/\gamma_0) \Gamma(2 + \kappa/\gamma_1) \\ &\times \int_0^\infty dr r W_{-\kappa/\gamma_0, \frac{1}{2}}(2\gamma_0 r) \left[\frac{\mu Z_\alpha}{m_\alpha} j_0\left(\frac{\mu}{m_\alpha} k_1 r\right) - \frac{\mu Z_C}{m_C} j_0\left(\frac{\mu}{m_C} k_1 r\right) \right] \\ &\times \left\{ \frac{\partial}{\partial r} \left[\frac{W_{-\kappa/\gamma_1, \frac{3}{2}}(2\gamma_1 r)}{r} \right] + 2 \frac{W_{-\kappa/\gamma_1, \frac{3}{2}}(2\gamma_1 r)}{r^2} \right\}, \end{aligned} \quad (9)$$

$$Y_{(c)}^{(l=1)} = \frac{1}{2\pi} y^{(0)} y^{(1)} \mu \left(\frac{Z_\alpha}{m_\alpha} - \frac{Z_C}{m_C} \right) \left[\frac{2\pi}{\mu} J_0^{div} - 2\kappa H(-i\kappa/\gamma_0) \right], \quad (10)$$

$$Y_{(d)}^{(l=1)} = -h^{(1)} y^{(0)} y^{(1)} \frac{Z_O}{\mu m_O}, \quad (11)$$

$$\begin{aligned} Y_{(a+b)}^{(l=2)} &= -\frac{2}{75\pi} y^{(0)} y^{(2)} \frac{\gamma_2^2}{\mu} \Gamma(1 + \kappa/\gamma_0) \Gamma(3 + \kappa/\gamma_2) \\ &\times \int_0^\infty dr r W_{-\kappa/\gamma_0, \frac{1}{2}}(2\gamma_0 r) \left[\frac{\mu Z_\alpha}{m_\alpha} j_1\left(\frac{\mu}{m_\alpha} k_2 r\right) + \frac{\mu Z_C}{m_C} j_1\left(\frac{\mu}{m_C} k_2 r\right) \right] \\ &\times \left\{ \frac{\partial}{\partial r} \left[\frac{W_{-\kappa/\gamma_2, \frac{5}{2}}(2\gamma_2 r)}{r} + 3 \frac{W_{-\kappa/\gamma_2, \frac{5}{2}}(2\gamma_2 r)}{r^2} \right] \right\}, \end{aligned} \quad (12)$$

$$Y_{(c)}^{(l=2)} = 0, \quad (13)$$

$$Y_{(d)}^{(l=2)} = +h^{(2)} y^{(0)} y^{(2)} \frac{Z_O}{\mu^2 m_O^2} k_2, \quad (14)$$

where $\Gamma(x)$, $j_l(x)$ ($l = 0, 1$), and $W_{\alpha, \beta}(x)$ are the gamma function, the spherical Bessel function, and the Whittaker function, respectively. μ is the reduced mass of α and ^{12}C , $\mu = m_\alpha m_C / (m_\alpha + m_C) = 2795$ MeV. γ_0 , γ_1 , and γ_2 are the binding momenta for 0_1^+ , 1_1^- , and 2_1^+ states of ^{16}O , respectively; $\gamma_l = \sqrt{2\mu B_l}$ with $l = 0, 1, 2$ where B_l are the binding energies. Thus, one has $\gamma_0 = 200.1$ MeV, $\gamma_1 = 15.88$ MeV, and $\gamma_2 = 37.00$ MeV. κ is the inverse of Bohr radius, $\kappa = \alpha_E Z_\alpha Z_C \mu$, where Z_α and Z_C (and Z_O in Eq. (14)) are the

number of protons in α and ^{12}C (and ^{16}O); $Z_\alpha = 2$ and $Z_C = 6$ (and $Z_O = 8$), respectively; thus, $\kappa = 245$ MeV. In addition, the function $H(\eta)$ in Eq. (10) reads

$$H(\eta) = \psi(i\eta) + \frac{1}{2i\eta} - \ln(i\eta), \quad (15)$$

where $\psi(z)$ is the digamma function and η is the Sommerfeld parameter. (We will mention the function J_0^{div} in Eq. (10) in the next subsection.)

One may notice that there are five constants, $\{y^{(0)}, y^{(1)}, y^{(2)}, h^{(1)}, h^{(2)}\}$, appearing in the amplitudes. Three of them, $y^{(0)}, y^{(1)}, y^{(2)}$, are determined by using the wave function normalization factors, and the remaining two parameters, $h^{(1)}$ and $h^{(2)}$, are fitted to the radiative decay data. Before fixing the parameters, we discuss the renormalization of infinities from one-loop diagrams in the next subsection.

3.2 Renormalization of the loop diagrams

The one-loop diagrams (a), (b), and (c) in Fig. 1 diverge. The divergent terms are subtracted by the counter terms, $h^{(1)}$ and $h^{(2)}$, in the diagram (d) in Fig. 1. For the diagrams (a) and (b), the r -space integrals in Eqs. (9) and (12) diverge: the log divergence appears in the limit where r goes to zero. In the previous work in Ref. [31], we introduced a sharp-cutoff r_C in the r -space integral for the radiative capture amplitude of $E1$ transition of $^{12}\text{C}(\alpha, \gamma)^{16}\text{O}$, and the divergent term was renormalized by the counter term, $h^{(1)}$. We found that the cutoff dependence was severe, and moreover, it was inconsistent with the regularization method, namely the dimensional regularization, which was applied to the calculation of diagram (c). In this work, we separate the r -space integrals in Eqs. (9) and (12) into two parts by introducing a cutoff parameter r_C , and the calculation of the log-diverging integral in the short-range part is carried out by employing the dimensional regularization in $d = 4 - 2\epsilon$ space-time dimensions, ignoring the other finite terms. Thus, a minor cutoff dependence remains in the numerical result. The log divergence of the short-range part is replaced as

$$\int_0^{r_C} \frac{dr}{r} \rightarrow \left(\frac{\mu_{DR}}{2}\right)^{2\epsilon} \int_0^{r_C} dr r^{-1+2\epsilon} = \frac{1}{2\epsilon} + \ln\left(\frac{\mu_{DR}}{2} r_C\right) + O(\epsilon), \quad (16)$$

where μ_{DR} is a scale parameter from the dimensional regularization. For the diagram (c) in Fig. 1, we employ dimensional regularization and calculate the loop integral in $d = 4 - 2\epsilon$ space-time dimension; one has the divergence term J_0^{div} as

$$J_0^{div} = \frac{\kappa\mu}{2\pi} \left[\frac{1}{\epsilon} - 3C_E + 2 + \ln\left(\frac{\pi\mu_{DR}^2}{4\kappa^2}\right) \right], \quad (17)$$

where C_E is the Euler-Mascheroni constant, $C_E = 0.5772\dots$.

We subtract the divergent terms being proportional to $1/(2\epsilon)$ as well as some constant terms by using the coupling constants, $h^{(1)}$ and $h^{(2)}$, as

$$h^{(1)} + \frac{\kappa\mu^2 m_O}{9\pi Z_O} \left(\frac{Z_\alpha}{m_\alpha} - \frac{Z_C}{m_C}\right) \left[\left(\frac{\mu_{DR}}{2}\right)^{2\epsilon} \int_0^{r_C} \frac{dr}{r^{1-2\epsilon}} - \frac{9\pi}{\kappa\mu} J_0^{div} \right]$$

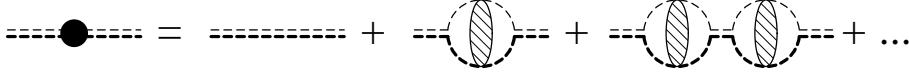


Figure 2: Diagrams for dressed ^{16}O propagator. A thick and thin double dashed line with and without a filled circle represents a dressed and bare ^{16}O propagator, respectively. See the caption of Fig. 1 as well.

$$= h_R^{(1)} + \frac{\kappa\mu^2 m_O}{9\pi Z_O} \left(\frac{Z_\alpha}{m_\alpha} - \frac{Z_C}{m_C} \right) \left[\ln \left(\frac{\mu_{DR}}{2} r_C \right) - 9 \ln \left(\frac{\mu_{DR}}{2\kappa} \right) \right], \quad (18)$$

$$h^{(2)} + \frac{2\kappa\mu^3 m_O^2}{75\pi Z_O} \left(\frac{Z_\alpha}{m_\alpha^2} + \frac{Z_C}{m_C^2} \right) \left(\frac{\mu_{DR}}{2} \right)^{2\epsilon} \int_0^{r_C} \frac{dr}{r^{1-2\epsilon}}$$

$$= h_R^{(2)} + \frac{2\kappa\mu^3 m_O^2}{75\pi Z_O} \left(\frac{Z_\alpha}{m_\alpha^2} + \frac{Z_C}{m_C^2} \right) \ln \left(\frac{\mu_{DR}}{2} r_C \right), \quad (19)$$

where $h_R^{(1)}$ and $h_R^{(2)}$ are the renormalized coupling constants and fitted to the experimental radiative decay rates in the next section.

3.3 Wave function normalization factors

The coefficients, $\{y^{(0)}, y^{(1)}, y^{(2)}\}$, appeared in the amplitudes can be fixed by using the wave function normalization factors, $\sqrt{\mathcal{Z}_l}$ with $l = 0, 1, 2$, which are related to the ANCs of 0_1^+ , 1_1^- , 2_1^+ states of ^{16}O for the two-body α - ^{12}C system. The relations between $y^{(l)}$ and $\sqrt{\mathcal{Z}_l}$ may be given as [32]⁴

$$y^{(l)} = \sqrt{2(2l+1)\pi\mu^{2l-1}} \sqrt{\mathcal{Z}_l}, \quad (20)$$

with $l = 0, 1, 2$. \mathcal{Z}_l are defined in the the inverse of dressed ^{16}O propagators, $D_l(p)$, for the two-body α - ^{12}C system, where p is the relative momentum between α and ^{12}C . Diagrams of dressed ^{16}O propagators are depicted in Fig. 2, and one has

$$\frac{1}{D_l(p)} = \frac{1}{K_l(p) - 2\kappa H_l(p)} = \frac{\mathcal{Z}_l}{E + B_l} + \dots, \quad (21)$$

where E is the kinetic energy of α and ^{12}C , $E = p^2/(2\mu)$, and B_l are the binding energies of bound states of ^{16}O as the α - ^{12}C two-body system. The dots denote finite terms at $E = -B_l$. The term, $-2\kappa H_l(p)$, is the Coulomb self-energy term from the one-loop diagram in Fig. 2, and one has

$$H_l(p) = W_l(p)H(\eta), \quad (22)$$

$$W_l(p) = \left(\frac{\kappa^2}{l^2} + p^2 \right) W_{l-1}(p), \quad W_0(p) = 1. \quad (23)$$

⁴The wave function normalization factors, $\sqrt{\mathcal{Z}_l}$ with $l = 0, 1, 2$, appear only in the initial and final states of reaction amplitudes. $y^{(l)}$ appearing in the intermediate states are represented, excluding $\sqrt{\mathcal{Z}_l}$, as $y^{(l)} = \sqrt{2(2l+1)\pi\mu^{2l-1}}$.

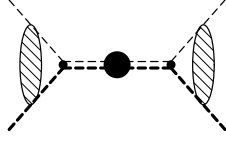


Figure 3: Diagram of the scattering amplitude. Shaded blobs in the initial and final states represent non-perturbative Coulomb interaction, namely, the Coulomb wave functions. See the captions of Figs. 1 and 2 as well.

The term, $K_l(p)$, is represented in terms of the effective range parameters as

$$K_l(p) = -\frac{1}{a_l} + \frac{1}{2}r_l p^2 - \frac{1}{4}P_l p^4 + Q_l p^6, \quad (24)$$

where one or two parameters of the effective range parameters are fixed by using the condition that the inverse of the propagator $D_l(p)$ vanishes at the binding momenta $\gamma_l = \sqrt{2\mu B_l}$, $D_l(i\gamma_l) = 0$. Thus, two parameters are fixed by using the binding energies of 0_1^+ and 0_2^+ states of ^{16}O for $l = 0$, and one parameter is fixed by using the binding energies of 1_1^- and 2_1^+ states of ^{16}O for $l = 1, 2$. We fix the scattering length and effective range a_0 and r_0 for $l = 0$ and the scattering lengths a_l for $l = 1, 2$. Thus, one has the inverse of propagators as [28, 29]

$$\begin{aligned} D_0(p) = & -\frac{1}{4} [\gamma_{01}^2 \gamma_{02}^2 + (\gamma_{01}^2 + \gamma_{02}^2)p^2 + p^4] P_0 \\ & + [-\gamma_{01}^4 \gamma_{02}^2 - \gamma_{01}^2 \gamma_{02}^4 - (\gamma_{01}^4 + \gamma_{01}^2 \gamma_{02}^2 + \gamma_{02}^4)p^2 + p^6] Q_0 \\ & - 2\kappa \left[\frac{\gamma_{02}^2 + p^2}{\gamma_{01}^2 - \gamma_{02}^2} H_0(i\gamma_{01}) - \frac{\gamma_{01}^2 + p^2}{\gamma_{01}^2 - \gamma_{02}^2} H_0(i\gamma_{02}) + H_0(p) \right], \end{aligned} \quad (25)$$

$$D_l(p) = \frac{1}{2}r_l(\gamma_l^2 + p^2) + \frac{1}{4}P_l(\gamma_l^4 - p^4) + Q_l(\gamma_l^6 + p^6) + 2\kappa [H_l(i\gamma_l) - H_l(p)], \quad (26)$$

with $l = 1, 2$: $\gamma_{01}(= \gamma_0)$ and γ_{02} are the bounding momenta of 0_1^+ and 0_2^+ states of ^{16}O , respectively; $\gamma_{02} = \sqrt{2\mu B_{02}}$, where B_{02} is the binding energy of the 0_2^+ state of ^{16}O as the two-body α - ^{12}C system, and one has $\gamma_{02} = 78.86$ MeV.

The other effective range parameters in Eqs. (25) and (26) are fitted to the phase shift data of elastic α - ^{12}C scattering. The elastic scattering amplitudes are calculated from a diagram depicted in Fig. 3. Expression of the S matrices, amplitudes, and fitted values of some parameters can be found in Ref. [30]. Thus, one may calculate the wave function normalization factors $\sqrt{\mathcal{Z}_l}$ from the inverse of propagators $D_l(p)$ in Eq. (21) as

$$\sqrt{\mathcal{Z}_l} = \left(2\mu \left| \frac{\partial D_l(p)}{\partial p^2} \right|_{p^2 = -\gamma_l^2} \right)^{-1/2}, \quad (27)$$

and through the relations in Eq. (20), those factors are multiplied to the amplitudes, as the coupling constants, $y^{(l)}$, for the initial 1_1^- or 2_1^+ state and final 0_1^+ state of ^{16}O .

In addition, the wave function normalization factors are related to ANCs through the formula derived by Iwinski, Rosenberg, and Spruch [33]:

$$|C_b|_l = \frac{\gamma_l^l}{l!} \Gamma(l+1 + \kappa/\gamma_l) \sqrt{2\mu Z_l}. \quad (28)$$

Now, we rewrite the amplitudes of radiative decay reactions in terms of the wave function renormalization factors as

$$Y_{(a+b)}^{(l=1)} = +\frac{16}{3\sqrt{3}} \sqrt{Z_{01} Z_1} \Gamma(1 + \kappa/\gamma_0) \Gamma(2 + \kappa/\gamma_1) \gamma_1^2 \\ \times \int_{r_C}^{\infty} dr e^{-(\gamma_0+\gamma_1)r} \gamma_0 \gamma_1 r^2 U(1 + \kappa/\gamma_0, 2, 2\gamma_0 r) \left[\frac{\mu Z_\alpha}{m_\alpha} j_0\left(\frac{\mu}{m_\alpha} k_1 r\right) - \frac{\mu Z_C}{m_C} j_0\left(\frac{\mu}{m_C} k_1 r\right) \right] \\ \times [(3 - \gamma_1 r) U(2 + \kappa/\gamma_1, 4, 2\gamma_1 r) - 2\gamma_1 r (2 + \kappa/\gamma_1) U(3 + \kappa/\gamma_1, 5, 2\gamma_1 r)], \quad (29)$$

$$Y_{(c)}^{(l=1)} = +\sqrt{3} \sqrt{Z_{01} Z_1} \mu \left(\frac{Z_\alpha}{m_\alpha} - \frac{Z_C}{m_C} \right) [-2\kappa H(-i\kappa/\gamma_0)], \quad (30)$$

$$Y_{(d)}^{(l=1)} = -2\sqrt{3} \pi \sqrt{Z_{01} Z_1} \frac{Z_O}{\mu m_O} \\ \times \left\{ h_R^{(1)} + \frac{\kappa \mu^2 m_O}{9\pi} \frac{Z_O}{Z_O} \left(\frac{Z_\alpha}{m_\alpha} - \frac{Z_C}{m_C} \right) \left[\ln\left(\frac{\mu_{DR}}{2} r_C\right) - 9 \ln\left(\frac{\mu_{DR}}{2\kappa}\right) \right] \right\}, \quad (31)$$

$$Y_{(a+b)}^{(l=2)} = -\frac{64\sqrt{5}}{75} \sqrt{Z_{01} Z_2} \gamma_2^3 \Gamma(1 + \kappa/\gamma) \Gamma(3 + \kappa/\gamma_2) \\ \times \int_{r_C}^{\infty} dr e^{-(\gamma_0+\gamma_2)r} \gamma_0 \gamma_2^2 r^3 U(1 + \kappa/\gamma_0, 2, 2\gamma_0 r) \left[\frac{\mu Z_\alpha}{m_\alpha} j_1\left(\frac{\mu}{m_\alpha} k_2 r\right) + \frac{\mu Z_C}{m_C} j_1\left(\frac{\mu}{m_C} k_2 r\right) \right] \\ \times [(5 - \gamma_2 r) U(3 + \kappa/\gamma_2, 6, 2\gamma_2 r) - 2\gamma_2 r (3 + \kappa/\gamma_2) U(4 + \kappa/\gamma_2, 7, 2\gamma_2 r)], \quad (32)$$

$$Y_{(c)}^{(l=2)} = 0, \quad (33)$$

$$Y_{(d)}^{(l=2)} = +2\sqrt{5} \pi \sqrt{Z_{01} Z_2} \frac{Z_O k_2}{\mu m_O^2} \left[h_R^{(2)} + \frac{2\kappa \mu^3 m_O^2}{75\pi} \frac{Z_O}{Z_O} \left(\frac{Z_\alpha}{m_\alpha^2} + \frac{Z_C}{m_C^2} \right) \ln\left(\frac{\mu_{DR}}{2} r_C\right) \right], \quad (34)$$

where we have also rewritten the Whittaker function, $W_{\kappa,\mu}(z)$, in terms of the Kummer function, $U(a, b, c)$. One may notice that the combinations for the ANCs appear in the amplitudes, $Y_{(a+b)}^{(l=1)}$ and $Y_{(a+b)}^{(l=2)}$, in Eqs. (29) and (32).

4. Numerical results

In this section, we first briefly review the calculation of the wave function renormalization factors, $\sqrt{Z_{01}}$, $\sqrt{Z_1}$, $\sqrt{Z_2}$, by fitting the effective range parameters to the experimental phase shift data of elastic α - ^{12}C scattering at low energies. In the following, we quote the values of the ANCs rather than those of $\sqrt{Z_l}$ because the ANCs are more reliable quantities for the other theoretical studies. Then, we fit the remaining two parameters, $h_R^{(1)}$ and $h_R^{(2)}$, to the radiative decay rates of sub-threshold 1^- and 2_1^+ states of ^{16}O . After fitting the parameters, there is no free parameter in $E1$ and $E2$ transitions of amplitudes of $^{12}\text{C}(\alpha, \gamma)^{16}\text{O}$, and we perform a parameter-free calculation of the astrophysical S factors for $E1$ and $E2$ transitions of $^{12}\text{C}(\alpha, \gamma)^{16}\text{O}$. We will see that the order of magnitude of the S factors compared to the experimental data is reproduced.

As discussed in the previous section, the coupling constants, $\{y^{(0)}, y^{(1)}, y^{(2)}\}$, are fixed by using the wave function normalization factors, $\sqrt{\mathcal{Z}_{01}}, \sqrt{\mathcal{Z}_1}, \sqrt{\mathcal{Z}_2}$, which are related to the ANCs through the relation in Eq. (28). In the previous work, we obtained the ANCs for 1_1^- and 2_1^+ states of ^{16}O as [30]

$$|C_b|_1 = 1.727(3) \times 10^{14} \text{ fm}^{-1/2}, \quad (35)$$

$$|C_b|_2 = 3.1(6) \times 10^4 \text{ fm}^{-1/2}, \quad (36)$$

by fitting the effective range parameters to the phase shift data [35]. We employ the fitted values of effective range parameters in TABLE II in Ref. [30] to calculate $\sqrt{\mathcal{Z}_1}$ and $\sqrt{\mathcal{Z}_2}$. The ANC of 1_1^- state agrees with the other results in literature while that of 2_1^+ state is about four times smaller than the other ones; the fit of effective range parameters for $l = 2$ is sensitive to the conditions of effective range parameters imposed on the low-energy region where the experimental phase shift data are not available [36].

To calculate $\sqrt{\mathcal{Z}_{01}}$, we need to fix the values of two effective range parameters, P_0 and Q_0 , in Eq. (25); we refit the parameters to the phase shift data including the $0_1^+, 0_2^+, 0_3^+, 0_4^+$ states of ^{16}O . Details of the fit of the parameters P_0 and Q_0 are discussed in Appendix B. Thus, we have the ANC of ground 0_1^+ state of ^{16}O as

$$|C_b|_{01} = 44.5(3) \text{ fm}^{-1/2}, \quad (37)$$

where the corresponding value of $y^{(0)}$ is $y^{(0)} = 0.355(3) \text{ MeV}^{-1/2}$. Those quantities, $|C_b|_{01}$ and $y^{(0)}$, are related through Eqs. (20) and (28); $|C_b|_{01} = \frac{\mu}{\sqrt{\pi}} \Gamma(1 + \kappa/\gamma_{01}) y^{(0)}$. It may be worth pointing out that this value of $|C_b|_{01}$ is close to that used in the recent R -matrix analysis for $^{12}\text{C}(\alpha, \gamma)^{16}\text{O}$ reported by deBoer et al., $|C_b|_{01} = 58 \text{ fm}^{-1/2}$ [8]. The reported values of the ANC, $|C_b|_{01}$, in literature are still scattered, 13.9(24) to 4000 $\text{fm}^{-1/2}$; see TABLE XVI in Ref. [8]. In addition, we fitted the values of $y^{(0)}$, along with the constant $h_R^{(1)}$ to the experimental data of S_{E1} factor of $^{12}\text{C}(\alpha, \gamma)^{16}\text{O}$ by using the sharp cutoff regularization scheme in the previous work [31] and had $y_0 = 0.253(9) - 2.249(84) \text{ MeV}^{-1/2}$ with the cutoff values $r_C = 0.01 - 0.35 \text{ fm}$. (The result of fitted values of $h_R^{(1)}$ and $y^{(0)}$ for the cutoff values $r_C = 0.01 - 0.10 \text{ fm}$ is included in Table 1.) The $y^{(0)}$ values are converted to the ANC as $|C_b|_{01} = 31.7(1) - 282(10) \text{ fm}^{-1/2}$. One may see that the value of ANC in Eq. (37) is reproduced at $r_C \simeq 0.05 \text{ fm}$. In this work, we fix the value of $y^{(0)}$ by using the ANC of ground 0_1^+ state of ^{16}O in Eq. (37) in the radiative decay amplitudes.

Now, the coupling constants $h_R^{(1)}$ and $h_R^{(2)}$ are fitted to the experimental data of radiative decay rates of 1_1^- and 2_1^+ states of ^{16}O [34],

$$\Gamma_1^{exp} = 0.055(3) \text{ eV}, \quad (38)$$

$$\Gamma_2^{exp} = 0.097(3) \text{ eV}, \quad (39)$$

as a function of the cutoff r_C where the scale parameter μ_{DR} is fixed as $\mu_{DR} = \Lambda_H$. The short-range part of integrals in the amplitudes, $Y_{(a+b)}^{(l=1)}$ and $Y_{(a+b)}^{(l=2)}$ in Eqs. (29) and (32), respectively, are replaced by the $1/r$ integrals in Eq. (16); the finite components are ignored and the cutoff dependence remains in the numerical results. The fitted values

r_C (fm)	$h_R^{(1)} \times 10^{-5}$ (MeV ³)	$h_R^{(1)}$ (MeV ³)[31]	$y^{(0)}$ (MeV ^{-1/2})[31]
0.005	2.503(2), 2.635(2)	–	–
0.01	2.626(2), 2.757(2)	$5.268(1) \times 10^5$	0.253(9)
0.035	2.775(2), 2.906(2)	$2.448(1) \times 10^5$	0.310(11)
0.05	2.825(2), 2.957(2)	$1.529(1) \times 10^5$	0.347(12)
0.10	2.957(2), 3.088(2)	$-0.070(1) \times 10^5$	0.495(18)

Table 1: Two values of $h_R^{(1)}$ in the second column are obtained by fitting to the radiative decay rate of 1_1^- state of ^{16}O , Γ_1^{exp} , as a function of the cutoff parameter r_C employing the dimensional regularization where the scale parameter μ_{DR} is fixed as $\mu_{DR} = \Lambda_H$. Values of $h_R^{(1)}$ and $y^{(0)}$ in the third and fourth columns are fitted values in the previous work [31], where $h_R^{(1)}$ and $y^{(0)}$ are treated as free parameters and fitted to the experimental data of S_{E1} factor of radiative α capture on ^{12}C employing the sharp cutoff regularization method.

r_C (fm)	$h_R^{(2)} \times 10^{-11}$ (MeV ⁴)
0.005	8.414(2), 8.627(2)
0.01	7.759(2), 7.971(2)
0.035	7.013(2), 7.226(2)
0.05	6.774(2), 6.986(2)
0.10	6.146(2), 6.359(2)

Table 2: Values of $h_R^{(2)}$ are obtained by fitting to the radiative decay rate of 2_1^+ state of ^{16}O , Γ_2^{exp} , as a function of the cutoff parameter r_C . See the caption of Table 1 as well.

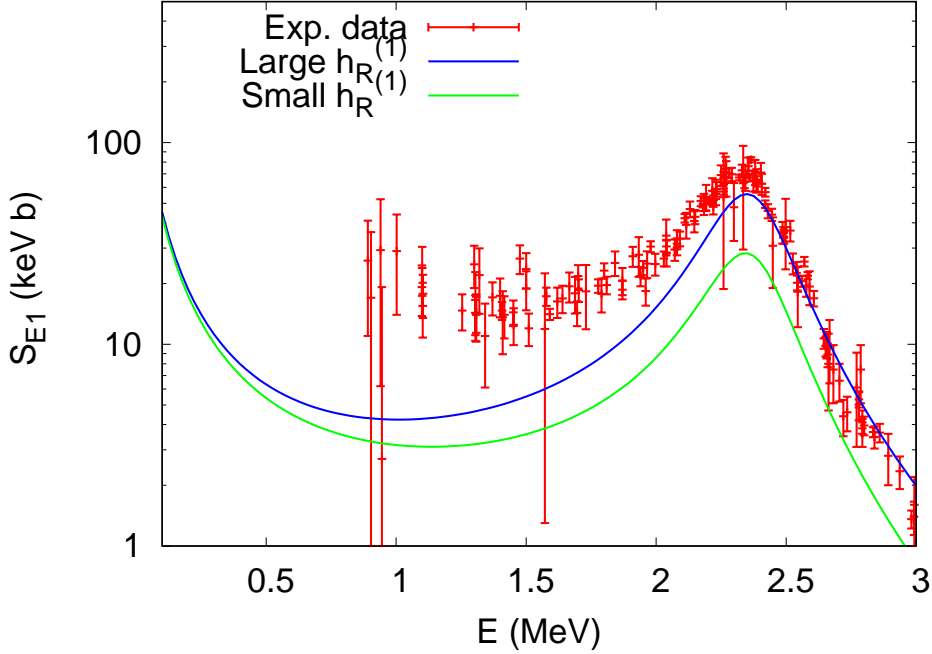


Figure 4: Curves of S_{E1} factor of radiative α capture on ^{12}C are plotted as a function of α - ^{12}C energy E in the center-of-mass frame by using the large and small values of $h_R^{(1)}$ at $r_C = 0.01$ fm in Table 1. Experimental data are displayed in the figure as well.

of $h_R^{(1)}$ and $h_R^{(2)}$ are presented in Tables 1 and 2, respectively. The fitted values of $h_R^{(1)}$ and $y^{(0)}$ in the previous work [31] are displayed in Table 1 as well. We find that there are two values of $h_R^{(1)}$ and $h_R^{(2)}$ with small error bars. This indicates a large cancellation between the amplitude of the loop diagrams and that of the counter term resulting in two same-size amplitudes with different signs. The cutoff dependence remains in the fitted values of $h_R^{(1)}$ and $h_R^{(2)}$ while that of $h_R^{(1)}$ becomes much milder than the previous fitted values obtained by means of the sharp cutoff regularization method.

In Figs. 4 and 5, we plot the astronomical S_{E1} and S_{E2} factors for $E1$ and $E2$ transitions of radiative α capture on ^{12}C as a function of the energy E of α - ^{12}C in the center-of-mass frame by using the large and small values of $h_R^{(1)}$ and $h_R^{(2)}$ with $r_C = 0.01$ fm in Tables 1 and 2, respectively. Experimental data of the S factors are displayed in the figures as well. A minor cutoff dependence is observed in the plots. (Figures for the other r_C values are suppressed.) We note that the curves plotted in the figures are not fitted to the data of S factors; those are parameter-free predictions. One can see that the curve of S_{E1} factor with the large value of $h_R^{(1)}$ in Fig. 4 and that of S_{E2} factor with the small value of $h_R^{(2)}$ in Fig. 5 relatively agree with the data.

In Fig. 4, the data on the high-energy side are reproduced better, but those on the low-energy side are not. It could be puzzling because a low-energy EFT is supposed to

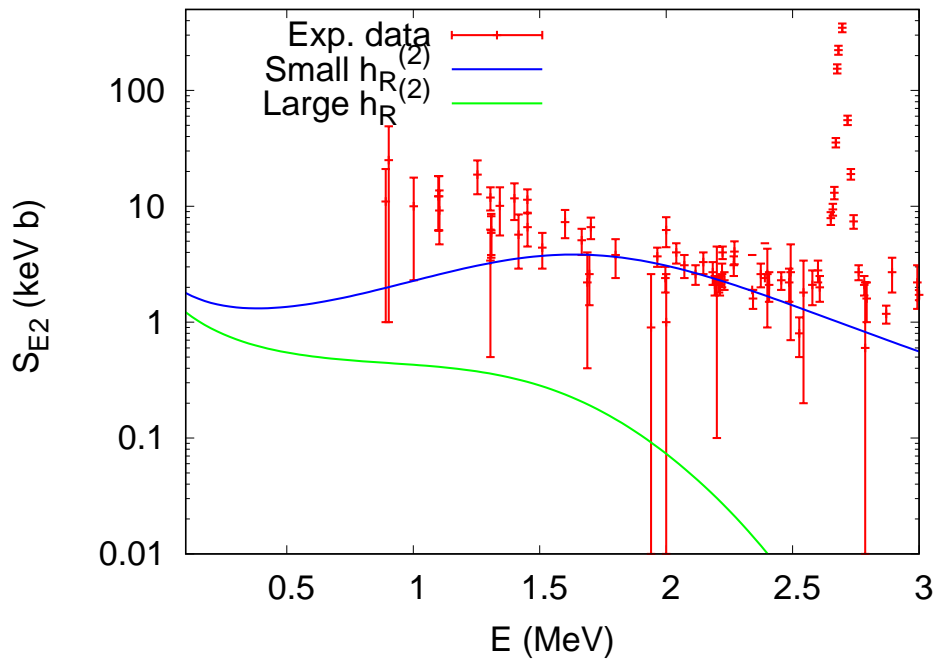


Figure 5: Curves of S_{E2} factor of radiative α capture on ^{12}C are plotted as a function of α - ^{12}C energy E in the center-of-mass frame by using the small and large values of $h_R^{(2)}$ at $r_C = 0.01$ fm in Table 2. Experimental data are displayed in the figure as well.

provide a better description of a reaction at lower energy. This expectation of EFT stems from the decoupling theorem [12], which describes how heavy particles at high energy enter into a low-energy theory. In the present case, however, the discrepancy between the fitted curves and the data appears at the low energy side of the resonant peak. Because a contribution from high energy will be more effective in the high energy side of resonant peak, to reproduce the shape of curves on the low energy side of resonance, it would be necessary to take account of higher order corrections to the $h_R^{(1)}$ term of $O\gamma O^*$ vertex function, which may play the role of form factor, a finite size effect of the nuclei involved in the reaction. The S_{E1} factor at $E_G = 0.3$ MeV is deduced as $S_{E1} = 11.2$ keV b with the large value of $h_R^{(1)}$ and $S_{E1} = 10.1$ keV b with the small value of $h_R^{(1)}$. Those values are significantly smaller than the value 86.3 keV b recently estimated by means of an R matrix analysis [8].

In Fig. 5, the sharp resonant peak at $E = 2.68$ MeV is not reproduced by the curves because the propagator of resonant 2_2^+ state of ^{16}O is not included. Moreover, the shape of the curve with a small value of $h_R^{(2)}$ at small energies, $E < 1.7$ MeV, is different from those one can find in literature; the curves of S_{E2} previously reported continuously increase as the energy decreases; no maximum and minimum points appear in the low-energy region. This is attributed to the fact that the effective range parameters for $l = 2$ are not well determined by using the phase shift data. It may be necessary to fit the effective range parameters by using the S_{E2} data. While, the S_{E2} factor at $E_G = 0.3$ MeV is deduced as $S_{E2} = 1.3$ keV b for the small value $h_R^{(2)}$ and $S_{E2} = 0.71$ keV b for the large value of $h_R^{(2)}$. Once again, those values are significantly smaller than the value 45.3 keV b recently estimated by an R matrix analysis [8].

5. Results and discussion

In the present work, we studied the radiative decay of sub-threshold 1_1^- and 2_1^+ states of ^{16}O within the cluster EFT. We, first, discussed an improvement of the regularization method: we employed the dimensional regularization method to calculate the log-divergent term, which was regularized by using the cutoff regularization method in the previous work. Because the finite terms below the cutoff r_C were ignored in the r -space integral, a minor cutoff dependence remains in the numerical result. In addition, we fixed the coupling constants, $y^{(0)}$, $y^{(1)}$, $y^{(2)}$, of $O^*\alpha C$ and $\alpha C O$ vertex functions for the initial and final states of ^{16}O by using the wave function normalization factors $\sqrt{\mathcal{Z}_l}$, equivalently the ANCs of 0_1^+ , 1_1^- , 2_1^+ states of ^{16}O . The values of $\sqrt{\mathcal{Z}_l}$ (or those of the ANCs) were deduced from the phase shift data of elastic α - ^{12}C scattering at low energies. After fixing the coupling constants, $y^{(0)}$, $y^{(1)}$, $y^{(2)}$, only one parameter, $h_R^{(1)}$ or $h_R^{(2)}$, remained in each of the radiative decay amplitudes, and we fitted them to the experimental data of decay rates of 1_1^- and 2_1^+ states of ^{16}O . We, then, perform a parameter-free calculation of S factors for $E1$ and $E2$ transitions of $^{12}\text{C}(\alpha, \gamma)^{16}\text{O}$ by using the fitted parameters in the present study and found that the order of the magnitude of S factors, compared to the experimental data, could be reproduced.

For previous estimates of the S factors in the literature, they are well summarized in Table IV in Ref. [8]. The reported values of S_{E1} factors at $E_G = 0.3$ MeV in the literatures

are scattered from 3 to 340 keV b with various sizes of the error bars, and those of S_{E2} factor at E_G are from 5 to 220 keV b with the various error bars as well. As mentioned above, we have $S_{E1} = 11.2$ and 10.1 keV b at E_G with the large and small values of $h_R^{(1)}$ and $S_{E2} = 1.3$ and 0.71 keV b with the small and large values of $h_R^{(2)}$. Those values are found to be small, an order of magnitude or two, compared to the large values of S factors at E_G reported in the literature. We note that those S factors we obtained at E_G are not fitted to the experimental values of S factors in the energy range, $E = 1$ to 3 MeV, displayed in Figs. 4 and 5, in which one can see that the plotted curves do not reproduce the experimental data well. To report a more reliable estimate of the S factors at E_G in cluster EFT, it would be anticipated to reproduce the data of S factors with a small χ^2 value.

The ANCs (or the wave function normalization factors) can be a model-independent quantity when a clear separation scale exists. For example, the asymptotic normalization factor of s -wave deuteron wave function works quite well [25, 37] where the deuteron binding energy is much smaller than the scale of NN interactions, namely the pion mass, m_π . Among the three ANCs which we employed in the present work, the ANC of 1_1^- state of ^{16}O could be a model-independent one because the binding energy is so small, $B_1 = 0.045$ MeV, compared to the separation scale, $\Delta E = 4$ MeV. Our estimate of the ANC for the 1_1^- state of ^{16}O turns out to be remarkably smaller, by about 20% (about one sigma difference with experimental error bars), than those obtained from the α -transfer reactions, $(^6\text{Li}, d)$ [38, 39]. Recently, a new deduction of the ANCs from the α -transfer reactions is reported by considering the new estimate of ANC of 1_1^+ state of ^6Li as a two-body d - α system [40], where the ANC of 1_1^+ state of ^6Li is obtained by means of an *ab initio* calculation of $\alpha(d, \gamma)^6\text{Li}$ capture rate and elastic d - α scattering at energies below 3 MeV [41]; the new value of ANC of 1_1^+ state of ^6Li turns out to be significantly larger than the value previously employed. The reported new value of the ANC of 1_1^- state of ^{16}O is now reduced and in better agreement with the result presented in Eq. (35).

Though the binding energy of 2_1^+ state of ^{16}O is also small, $B_2 = 0.245$ MeV, there is a large uncertainty, at least a factor of 2, to deduce the ANC of 2_1^+ state of ^{16}O , mainly because of the tiny phase shifts at energies below the resonant 2_2^+ state of ^{16}O . (The difficulty to fix the ANC of 2_1^+ state of ^{16}O from the phase shift of elastic α - ^{12}C scattering is discussed in Appendix in Ref. [30].) The ambiguity in the value of ANC could be compensated by the fitted value of $h_R^{(2)}$ in the radiative decay amplitudes. However, as mentioned before, the energy dependence of S factor for $E2$ transition of $^{12}\text{C}(\alpha, \gamma)^{16}\text{O}$ is different from that of the experimental data of S factor in Fig. 5. It may be necessary to fix the effective range parameters for $l = 2$ by using the data of S factor of $E2$ transition or those of the other reactions.

The use of the ANC of ground 0_1^+ state of ^{16}O is questionable, though it was encouraging to see that the value of ANC of 0_1^+ state of ^{16}O obtained in Eq. (37) is close to that employed in the recent R -matrix analysis [8] as well as those fitted to the S factor of $E1$ transition of $^{12}\text{C}(\alpha, \gamma)^{16}\text{O}$, as discussed above. Because the length scale between α and ^{12}C in the ground state is quite short, $\gamma_0^{-1} \simeq 1$ fm (and γ_0 is larger than the large scale of the theory, Λ_H , $\gamma_0 > \Lambda_H$), it seems that a model dependence in the ANC of 0_1^+ state of

$m_{O^*(1_1^-)}$	14902.196426(140) MeV
$m_{O^*(2_1^+)}$	14901.9967(6) MeV
m_O	14895.079576 MeV
m_α	3727.379 MeV
m_C	11174.862 MeV

Table 3: Masses of nuclei in the unit of MeV, which are used in the present work.

^{16}O is inevitable. Only the order of magnitude of the ANC may be reliable, and thus, it would be practical to fit the ANC (or the coupling constant $y^{(0)}$) to the data of S factors together with the coefficients of contact terms, $h_R^{(1)}$ and $h_R^{(2)}$.

We found the double values of fitted parameters, $h_R^{(1)}$ and $h_R^{(2)}$ in Tables 1 and 2. As mentioned, this implies a large cancelation between the contributions from loop diagrams and counter terms. The size of the radiative decay amplitudes may be estimated by using a relation, $[h_R^{(l)}(L) - h_R^{(l)}(S)]/[h_R^{(l)}(L) + h_R^{(l)}(S)]$, where $h_R^{(l)}(L/S)$ represent the large/small values of $h_R^{(l)}$, and we have 0.025 for $l = 1$ and 0.013 for $l = 2$ by using the values at $r_C = 0.01$ fm in the tables. Two orders of magnitude large values of $h_R^{(1)}$ and $h_R^{(2)}$ are obtained, compared to the size of amplitudes for the radiative decay. This could be a similar situation to that for the modification of counting rules introduced in the effective range parameters of elastic α - ^{12}C scattering at low energies. Thus, we might need to introduce higher-order corrections to the $h_R^{(1)}$ and $h_R^{(2)}$ contact vertex functions as counter terms. As discussed above, such corrections would play a role of the form factor, which describe a finite size effect of ^{16}O .

Acknowledgements

This work was supported by the National Research Foundation of Korea (NRF) grant funded by the Korean government (MSIT) (No. 2019R1F1A1040362 and 2022R1F1A1070060).

Appendix A

Masses of $^{16}\text{O}^*(1_1^-)$, $^{16}\text{O}^*(2_1^+)$, and ^{16}O as well as α and ^{12}C are presented in Table 3, and the mass differences (excited energies) of 1_1^- and 2_1^+ states with respect to the ground 0_1^+ state of ^{16}O are [34]

$$\Delta_1 = m_{O^*(1_1^-)} - m_O = 7.11685(14) \text{ MeV}, \quad (40)$$

$$\Delta_2 = m_{O^*(2_1^+)} - m_O = 6.9171(6) \text{ MeV}. \quad (41)$$

At the rest frame for $^{16}\text{O}^*$, the 1_1^- and 2_1^+ states of ^{16}O decay to the ground state of ^{16}O by emitting a photon. The energy-momentum conservation including the terms up to $1/m_O$ corrections reads

$$\Delta_l = k_l + \frac{1}{2m_O} k_l^2 \simeq k_l + \frac{1}{2m_O} \Delta_l^2, \quad (42)$$

with $l = 1, 2$. The magnitudes of photon momenta k_1 and k_2 (or photon energies) are obtained as

$$k_1 = \Delta_1 - \frac{1}{2m_O} \Delta_1^2 = 7.1152(1) \text{ MeV}, \quad (43)$$

$$k_2 = \Delta_2 - \frac{1}{2m_O} \Delta_2^2 = 6.9155(6) \text{ MeV}, \quad (44)$$

where $\Delta_1^2/(2m_O) \simeq 1.7 \times 10^{-3} \text{ MeV}$ and $\Delta_2^2/(2m_O) \simeq 1.6 \times 10^{-3} \text{ MeV}$.

Thus, one has the spin-averaged decay rates as

$$\Gamma_l = \frac{k_l}{2\pi} \frac{1}{2S_{O^*(l)} + 1} \sum_{spins} |A^{(l)}|^2, \quad (45)$$

where $S_{O^*(1^-)} = 1$ and $S_{O^*(2^+)} = 2$, and $A^{(l)}$ are the radiative decay amplitudes which we calculate from the effective Lagrangian.

Appendix B

In the previous works, we calculated the ANCs of 0_1^+ and 0_2^+ states of ^{16}O , not including the resonant states of ^{16}O , by fitting the parameters to the phase shift of elastic α - ^{12}C scattering for $l = 0$ below the energy of the first resonant 0_3^+ state [29]. We also calculated the ANC of 0_2^+ state of ^{16}O including the resonant 0_3^+ and 0_4^+ states of ^{16}O (but not including the 0_1^+ state of ^{16}O) by fitting the parameters to the phase shift data below the p - ^{15}N breakup energy [30]. In this appendix, we discuss the derivation of the ANC of the ground 0_1^+ state of ^{16}O including the excited 0_2^+ bound state and 0_3^+ and 0_4^+ resonant states of ^{16}O by fitting the parameters to the phase shift below the p - ^{16}N breakup energy.

We employ the expression of S matrix for elastic α - ^{12}C scattering at low energies for $l = 0$ in terms of the effective range parameters in Eq. (28) in Ref. [30]:

$$e^{2i\delta_0} = \frac{K_0(p) - 2\kappa \text{Re}H_0(p) + ipC_\eta^2 \prod_{i=3}^4 \frac{E - E_{R(0i)} + R_{(0i)}(E) - i\frac{1}{2}\Gamma_{(0i)}(E)}{E - E_{R(0i)} + R_{(0i)}(E) + i\frac{1}{2}\Gamma_{(0i)}(E)}}{K_0(p) - 2\kappa \text{Re}H_0(p) - ipC_\eta^2 \prod_{i=3}^4 \frac{E - E_{R(0i)} + R_{(0i)}(E) - i\frac{1}{2}\Gamma_{(0i)}(E)}{E - E_{R(0i)} + R_{(0i)}(E) + i\frac{1}{2}\Gamma_{(0i)}(E)}}, \quad (46)$$

where δ_0 is the phase shift of elastic α - ^{12}C scattering for $l = 0$, and $K_0(p) = D_0(p) + 2\kappa H_0(p)$; $D_0(p)$ is given in Eq. (25) and has two zeros for the 0_1^+ and 0_2^+ bound states, $D_0(i\gamma_{01}) = 0$ and $D_0(i\gamma_{02}) = 0$. Furthermore,

$$R_{(0i)}(E) = a_{(0i)}(E - E_{R(0i)})^2 + b_{(0i)}(E - E_{R(0i)})^3, \quad (47)$$

$$\Gamma_{(0i)}(E) = \Gamma_{R(0i)} \frac{pC_\eta^2}{p_r C_{\eta_r}^2}, \quad C_\eta^2 = \frac{2\pi\eta}{e^{2\pi\eta} - 1}, \quad (48)$$

where $E_{R(0i)}$ and $\Gamma_{R(0i)}$ are resonant energies and widths, and $a_{(0i)}$ and $b_{(0i)}$ are the coefficients of second order $(E - E_{R(0i)})^2$ and third order $(E - E_{R(0i)})^3$ contributions in the Breit-Wigner-like expression for the resonant states. p_r are resonant momenta, $p_r = \sqrt{2\mu E_{R(0i)}}$ and $\eta_r = \kappa/p_r$. (We suppress the index i for p_r and η_r .)

After including the two zeros in $D_0(p)$ in Eq. (25), we have 10 parameters, $\{P_0, Q_0; E_{R(03)}, \Gamma_{R(03)}, a_{(03)}, b_{(03)}; E_{R(04)}, \Gamma_{R(04)}, a_{(04)}, b_{(04)}\}$, in general, however, we exclude $a_{(03)}$

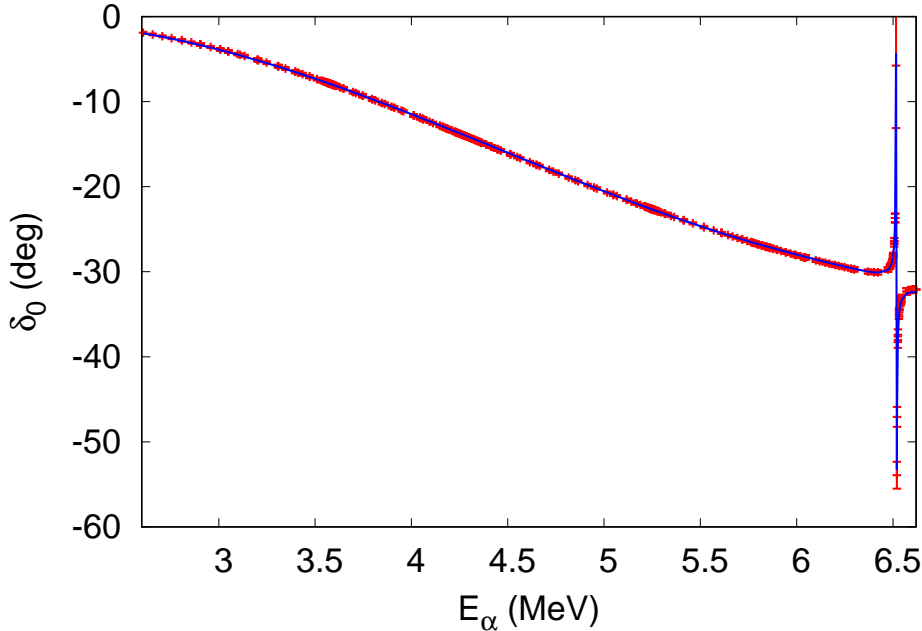


Figure 6: Phase shift δ_0 of elastic α - ^{12}C scattering for $l = 0$ is plotted as a function of E_α by using the fitted parameters, where E_α is the α energy in the lab frame. The experimental data are displayed in the figure as well.

and $b_{(03)}$ from the fit because the resonant 0_3^+ state is so sharp and the fit is insensitive to $a_{(03)}$ and $b_{(03)}$. We fix $E_{R(04)}$ and $\Gamma_{R(04)}$ by using the experimental data, $E_{R(04)}^{exp} = 6.870(15)$ MeV and $\Gamma_{R(04)}^{exp} = 185(35)$ keV for the 0_4^+ state [34] because its peak does not appear in the data; it provides a background contribution from high energy, where $a_{(04)}$ and $b_{(04)}$ describe the high energy tale from the 0_4^+ state of ^{16}O . Thus, we have 6 parameters, $\{P_0, Q_0; E_{R(03)}, \Gamma_{R(03)}; a_{(04)}, b_{(04)}\}$, to fit the phase shift data.

The six parameters are fitted to the phase shift data of elastic α - ^{12}C scattering measured at $E_\alpha = 2.6 - 6.62$ MeV, reported by Tischhauser et al. [35], where E_α is the α energy in the lab frame, and we have

$$P_0 = -0.03452(2) \text{ fm}^3, \quad Q_0 = 0.001723(7) \text{ fm}^5, \quad (49)$$

$$E_{R(03)} = 4.8883(1) \text{ MeV}, \quad \Gamma_{R(03)} = 1.35(3) \text{ keV}, \quad (50)$$

$$a_{(04)} = 0.756(7) \text{ MeV}^{-1}, \quad b_{(04)} = 0.167(4) \text{ MeV}^{-2}, \quad (51)$$

where the chi-square per the number of data is $\chi^2/N = 0.10$: N is the number of data, $N = 252$. The fitted values of $E_{R(03)}$ and $\Gamma_{R(03)}$ agree well with the experimental values, $E_{R(03)}^{exp} = 4.887(2)$ MeV and $\Gamma_{R(03)}^{exp} = 1.5(5)$ keV [34].

In Fig. 6, we plot the phase shift, δ_0 , using the fitted parameters and include the experimental data in the figure. One can see that the plotted curve reproduces the data

	w/o $0_3^+, 0_4^+$ [29]	w/o 0_1^+ [30]	This work
$ C_b _{01}(\text{fm}^{-1/2})$	44(2)	–	44.5(3)
$ C_b _{02}(\text{fm}^{-1/2})$	605(44)	370(25)	621(9)

Table 4: ANCs of 0_1^+ and 0_2^+ states of ^{16}O , $|C_b|_{01}$ and $|C_b|_{02}$, respectively, for two-body α - ^{12}C bound state. Values in the second column are the result not including the resonant 0_3^+ and 0_4^+ state in the parameter fit [29]. A value in the third column is the result not including the ground 0_1^+ state [30]. Values in the last column are the result of this work.

well. In Table 4, we display the values of ANCs of 0_1^+ and 0_2^+ states of ^{16}O for the two-body α - ^{12}C state, $|C_b|_{01}$ and $|C_b|_{02}$, respectively, calculated by using the values of effective range parameters, P_0 and Q_0 , in Eq. (49). We also display the ANCs by using the parameters fitted not including the resonant 0_3^+ and 0_4^+ states and those not including the ground 0_1^+ state in the table. One can see that the results of this work and those not including the resonant 0_3^+ and 0_4^+ states are in good agreement within the error bars, while the result of ANC for 0_2^+ state obtained not including the ground 0_1^+ state is small, about 60% of that of this work.

References

- [1] W. A. Fowler, “Experimental and theoretical nuclear astrophysics: the quest for the origin of the elements,” *Rev. Mod. Phys.* **56**, 149 (1984).
- [2] T. A. Weaver and S. E. Woosley, “Nucleosynthesis in massive stars and the $^{12}\text{C}(\alpha,\gamma)^{16}\text{O}$ reaction rate,” *Phys. Rep.* **227**, 65 (1993).
- [3] G. Imbriani et al., “The $^{12}\text{C}(\alpha,\gamma)^{16}\text{O}$ reaction rate and the evolution of stars in the mass range $0.8 \leq M/M_\odot \leq 25$,” *Astr. Jour.* **558**, 903 (2001).
- [4] J. José, *Stellar Explosions, Hydrodynamics and Nucleosynthesis*, (CRC Press, first issued in paperback 2020).
- [5] L. R. Buchmann and C. A. Barnes, “Nuclear reactions in stellar helium burning and later hydrostatic burning states,” *Nucl. Phys. A* **777**, 254 (2006).
- [6] A. Coc et al., “Recent results in nuclear astrophysics,” *Eur. Phys. J. A* **51**: 34 (2015).
- [7] C. A. Bertulani and T. Kajino, “Frontiers in nuclear astrophysics,” *Prog. Part. Nucl. Phys.* **89**, 56 (2016).
- [8] R. J. deBoer et al., “The $^{12}\text{C}(\alpha,\gamma)^{16}\text{O}$ reaction and its implications for stellar helium burning,” *Rev. Mod. Phys.* **89**, 035007 (2017), and references therein.

- [9] S.-I. Ando, “Cluster effective field theory and nuclear reactions,” *Eur. Phys. J. A* **57**: 17 (2021).
- [10] S. Weinberg, “Phenomenological Lagrangians,” *Physica A* **96**, 327 (1979).
- [11] P. F. Bedaque and U. van Kolck, “Effective field theory for few-nucleon systems,” *Annu. Rev. Nucl. Part. Sci.* **52**, 339 (2002).
- [12] J. F. Donoghue, E. Golowich, and B. R. Holstein, *Dynamics of the Standard Model* (Second Edition, Cambridge University Press, 2014).
- [13] B. A. Gelman, “Narrow resonances and short-range interactions,” *Phys. Rev. C* **80**, 034005 (2009).
- [14] J. B. Habashi, S. Fleming, and U. van Kolck, “Nonrelativistic effective field theory with a resonance field,” *Eur. Phys. J. A* **57**: 169 (2021).
- [15] J. W. Chen and M. J. Savage, “ $np \rightarrow d\gamma$ for big-bang nucleosynthesis,” *Phys. Rev. C* **60**, 065205 (1999).
- [16] G. Rupak, “Precision calculation of $np \rightarrow d\gamma$ cross section for big-bang nucleosynthesis,” *Nucl. Phys. A* **678**, 405 (2000).
- [17] S. Ando, R. H. Cyburt, S. W. Hong, and C. H. Hyun, “Radiative neutron capture on a proton at big-bang nucleosynthesis energies,” *Phys. Rev. C* **74**, 025809 (2006).
- [18] X. Kong and F. Ravndal, “Proton-proton fusion in leading order of effective field theory,” *Nucl. Phys. A* **656**, 421 (1999).
- [19] M. Butler and J.-W. Chen, “Proton-proton fusion in effective field theory to fifth order,” *Phys. Lett. B* **520**, 87 (2001).
- [20] S. Ando et al., “Proton-proton fusion in pionless effective field theory,” *Phys. Lett. B* **668**, 187 (2008).
- [21] M. Butler, J.-W. Chen, and X. Kong, “Neutrino-deuteron scattering in effective field theory at next-to-next-to-leading order,” *Phys. Rev. C* **63**, 035501 (2001).
- [22] S.-I. Ando, Y.-H. Song, and C. H. Hyun, “Neutrino-deuteron reactions at solar neutrino energies in pionless effective field theory with dibaryon fields,” *Phys. Rev. C* **101**, 054001 (2020).
- [23] D. B. Kaplan, “More effective field theory for nonrelativistic scattering,” *Nucl. Phys. B* **494**, 471 (1997).
- [24] S. R. Beane and M. J. Savage, “Rearranging pionless effective field theory,” *Nucl. Phys. A* **694**, 511 (2001).

- [25] S.-I. Ando and C. H. Hyun, “Effective field theory of the deuteron with dibaryon field,” *Phys. Rev. C* **72**, 014008 (2005).
- [26] H. A. Bethe, “Theory of the effective range in nuclear scattering,” *Phys. Rev.* **76**, 38 (1949).
- [27] S.-I. Ando, “Elastic α - ^{12}C scattering at low energies in cluster effective field theory,” *Eur. Phys. J. A* **52**: 130 (2016).
- [28] S.-I. Ando, “Elastic α - ^{12}C scattering at low energies with the bound states of ^{16}O in effective field theory,” *Phys. Rev. C* **97**, 014604 (2018).
- [29] S.-I. Ando, “Elastic α - ^{12}C scattering with the Ground State of ^{16}O at low energies in Effective Field Theory,” *J. Korean Phys. Soc.* **73**, 1452 (2018).
- [30] S.-I. Ando, “ S matrices of elastic α - ^{12}C scattering at low energies in effective field theory,” *Phys. Rev. C* **107**, 045808 (2023).
- [31] S.-I. Ando, “ S_{E1} factor of radiative α capture on ^{12}C in cluster effective field theory,” *Phys. Rev. C* **100**, 015807 (2019).
- [32] H. W. Griebhammer, “Improved convergence in the three-nucleon system at very low energies,” *Nucl. Phys. A* **744**, 192 (2004).
- [33] Z. R. Iwinski, L. Rosenberg, and L. Spruch, “Radiative capture estimates via analytic continuation of elastic scattering data, and the solar-neutrino problem,” *Phys. Rev. C* **29**, 349 (1984).
- [34] D. R. Tilley, H. R. Weller, and C. M. Cheves, “Energy levels of light nuclei $A = 16 - 17$,” *Nucl. Phys. A* **564**, 1 (1993).
- [35] P. Tischhauser et al., “Measurement of elastic $^{12}\text{C}+\alpha$ scattering: Details of the experiment, analysis, and discussion of phase shifts,” *Phys. Rev. C* **79**, 055803 (2009).
- [36] S.-I. Ando, “Elastic α - ^{12}C scattering at low energies with the resonant 2_2^+ and 2_3^+ states of ^{16}O ,” *Phys. Rev. C* **105**, 064603 (2022).
- [37] T. Ericson and W. Weise, *Pions and Nuclei*, (Oxford University Press, 1988).
- [38] C. R. Brune et al., “Sub-Coulomb α transfer on ^{12}C and the $^{12}\text{C}(\alpha,\gamma)^{16}\text{O}$ S factor,” *Phys. Rev. Lett.* **83**, 4025 (1999).
- [39] M. L. Avila et al., “Constraining the 6.05 MeV 0^+ and 6.16 MeV 3^- cascade transitions in the $^{12}\text{C}(\alpha,\gamma)^{16}\text{O}$ reaction using the asymptotic normalization coefficients,” *Phys. Rev. Lett.* **114**, 071101 (2015).
- [40] C. Hebborn, M. L. Avila, K. Kravvaris, G. Potel, and S. Quaglioni, “Impact of the ^6Li asymptotic normalization constant onto α -induced reactions astrophysical interest,” arXiv:2307.05636 [nucl-th] (2023).

- [41] C. Hebborn, G. Hupin, K. Kravvaris, S. Quaglioni, P. Navrátil, and P. Gysbers, “*Ab initio* prediction of the ${}^4\text{He}(d,\gamma){}^6\text{Li}$ big bang radiative capture,” *Phys. Rev. Lett.* **129**, 042503 (2022).